

USR NEWSLETTER

Lawrence Berkeley Laboratory, University of California
Meson Science Laboratory, University of Tokyo, Japan

= EDITORS: _____

K. M. Crowe	LBL
A. M. Portis	UC Berkeley
T. Yamazaki	U of Tokyo

= SECRETARY: _____

S. S. Rosenblum	LBL
-----------------	-----

= CONTRIBUTING EDITORS: _____

J. H. Brewer	TRIUMF
F. N. Gygax	SIN
V. W. Hughes	Yale
C. Kittel	UC Berkeley
W. J. Kossler	William and Mary
P. M. Platzman	Bell Labs
A. Schenck	SIN

DEFINITION OF μ SR

μ SR stands for Muon Spin Relaxation, Rotation, Resonance, Research, or what have you. The intention of the mnemonic acronym is to draw attention to the analogy with NMR and ESR, the range of whose applications is well known. Any study of the interactions of the muon spin by virtue of the asymmetric decay is considered μ SR, but this definition is not intended to exclude any peripherally related phenomena, especially if relevant to the use of the muon's magnetic moment as a delicate probe of matter.

No. 33

May 12, 1987

TABLE OF CONTENTS

Page

Long-Time Spin Relaxation in Zero-Field

R. Kubo, N. Endo, S. Kambara, M. Shimizu,
M. Fujii, and H. Takano 1830

Determination of the Electronic Structure of Anomalous
Muonium in GaAs from Nuclear Hyperfine Interactions

R.F. Kiefl, M. Celio, T.L. Estle, G.M. Luke, S.R. Kreitzman,
J.H. Brewer, D.R. Noakes, E.J. Ansaldo, and K. Nishiyama 1843

Zero Field μ^+ Spin Relaxation in $Cd_{1-x}Mn_xTe$
Diluted Magnetic Semiconductors

E.J. Ansaldo, D.R. Noakes, R. Keitel, S.R. Kreitzman,
J.H. Brewer, and J.K. Furdyna 1853

Magnetic Penetration Depth and Flux-Pinning Effects
in High- T_c Superconductor $La_{1.85}Sr_{0.15}CuO_4$

G. Aeppli, E.J. Ansaldo, J.H. Brewer, R.J. Cava,
R.F. Kiefl, S.R. Kreitzman, G.M. Luke, and D.R. Noakes 1864

RCDC Bibliographic Database 1879

Long-Time Spin Relaxation in Zero-Field

Ryogo Kubo, Naohiko Endo, Shiro Kambara, Mitsuaki Shimizu

Masataka Fijii, and Hiroshi Takano

Department of Physics, Faculty of Science and Technology

Keio University

1-14 Hiyoshi 3-Chome Kohokuku Yokohama 223 Japan

Abstract

The long-time tail of the Kubo-Toyabe relaxation function of spin polarization in zero-field is examined by a variational method and a numerical simulation. The asymptotic exponential decay was found to be of the form, $0.2362 \exp(-1.562 \nu t)$, where ν is the decay constant of the perturbing Gaussian random field. This decay constant is shown to be determined by the lowest eigenvalue of a confluent differential equation.

§ 1. INTRODUCTION.

In 1966, Kubo and Toyabe [1,2] studied a stochastic model for low field resonance and relaxation of spins randomly modulated by a local field which is modelled by a Gaussian Markoffian process. The field applied externally is supposed to be weak in comparison with the magnitude of the local field or even to be zero. Accordingly the local field can no longer be regarded as a weak perturbation to the Zeeman energy. Therefore a non-perturbative method is

MASTER

DISTRIBUTION OF THIS DOCUMENT IS UNLIMITED

EAB

needed in order to calculate relaxation functions or the spin resonance spectra. The Gaussian Markoffian assumption made it possible to compute these functions. The motivation of the work was purely academic, because spin resonance or relaxation is usually studied experimentally by applying a strong external field. Some years later, it was discovered that the zero-field relaxation is a powerful method for studying a condensed matter by the muon-depolarization experiment [3]. Since that time the Kubo-Toyabe theory became a useful tool for analysis of μ SR experiments.

The important point is that the zero- or low field spin relaxation shows a long-time tail if the modulation rate, which is denoted by ν throughout this paper, of the local field is small in comparison with the magnitudes of the modulation, which will be denoted Δ . When ν is zero, namely when the local field is regarded as static, the Kubo-Toyabe function of relaxation starts from the initial value equal to 1, decreases with time, passing through a minimum and then rises to $1/3$ and stays there to infinite time. If ν is finite but small, then the $1/3$ tail decays in time. The decay constant was estimated by Toyabe [2] to be 4ν by a simple variational method, but this was suspected to be too large. If the Gaussian process model is replaced by a strong collision model, the decay constant is simply equal to $2\nu/3$ [4]. Analyses of experiments are usually done assuming this decay rate.

In this paper, the variational formulation is carried out to higher approximations. First the calculation was made numerically and the long-time tail was found to be given by a sum of finite terms, up to six terms, each of which has a characteristic decay. Then we show that the problem is analytically treated by expanding the solution in terms of eigenfunctions of a confluent differential operator and find that the relaxation function is expressed by a series of exponential decay functions. The decay constants are given by the formula,

$$\gamma_n = (1.56155 + 2n) \nu$$

with integers n . We also made a numerical simulation of spin motion randomly modulated by a Gaussian process. The result of the simulation was in a good accord with the variational calculation.

§ 2. The Basic Equation of Spin relaxation.

The stochastic equation of motion of a spin in a random magnetic field is written as

$$\frac{d}{dt} \vec{m}(t) = (\vec{\omega}_0 + \vec{r}(t)) \times \vec{m}(t) \quad (1)$$

where ω_0 represents a constant magnetic field and $\vec{r}(t) = (x(t), y(t), z(t))$ is a random field, which we assume here to be a Gaussian Markoffian process. For simplicity, we take their variance equal to unity. Namely the magnetic fields are all scaled by the variance Δ . The transition probability $P(\vec{r}, t)$ for $\vec{r}(t)$ then follows the Fokker-Planck equation

$$\begin{aligned} \frac{\partial}{\partial t} P(\vec{r}, t) &= \Gamma P(\vec{r}, t) \\ &= \nu \vec{\nabla}(\vec{r} + \vec{\nabla}) P(\vec{r}, t) \end{aligned} \quad (2)$$

It has been shown [5] that the relaxation function is determined by the equation

$$\begin{aligned} \left(\frac{d}{dt} - \Gamma\right) M_x + (z + \omega_0) M_y - y M_z &= 0 \\ -(z + \omega_0) M_x + \left(\frac{d}{dt} - \Gamma\right) M_y + x M_z &= 0 \\ y M_x - x M_y - \left(\frac{d}{dt} - \Gamma\right) M_z &= 0 \end{aligned} \quad (3)$$

where we have chosen the z -axis along the constant magnetic field and denoted the corresponding Zeeman frequency by ω_0 . M_x , M_y and M_z are functions of the

variables x , y , z and t . The initial condition at $t = 0$ is chosen to be

$$M_x = M_y = 0$$

and

$$M_z(\vec{r}, 0) = P_0(r) = (2\pi)^{-3/2} e^{-r^2/2} \quad (4)$$

Namely we assume that spins are polarized initially in the z -direction and the local field distribution is the equilibrium. The expectation of the z -component of spins is obtained by integrating the function $M_z(\vec{r}, t)$ over \vec{r} .

This is the relaxation (depolarization) function, which will be denoted later by $G(t)$. Hereafter we consider the zero-field relaxation and assume ω_0 to be zero. By performing Laplace transformation and by eliminating the components M_x and M_y , we obtain

$$\left[(p - \Gamma + \frac{1}{2}(x-iy) \frac{1}{p - \Gamma - iz} (x-iy) + \frac{1}{2}(x+iy) \frac{1}{p - \Gamma + iz}) \right] M_z[\vec{x}, p] = P_0(\vec{x}) \quad (5)$$

where $M_z[\vec{r}, p]$ is the Laplace transform of $M_z(\vec{r}, t)$. It is difficult to obtain the solution of this equation in a closed analytical form. So, Kubo and Toyabe made numerical calculations by expanding the solution in Hermite polynomials which are the eigenfunctions of the operator Γ .

Here we consider the long-time tail by assuming the rate ν is small in comparison with $\Delta (= 1)$. This can be done by expanding the fractional operators in Eq. (5) to the first power of $(p - \Gamma) / z$, since the long-time behaviour is determined by small values of the Laplace parameter p of the order of ν , whereas the variable z is order one. It is convenient to transform the equation by writing

$$F(\vec{x}, s) = M_z[\vec{x}, p] \exp(-x^2/4) \quad (6)$$

and

$$\begin{aligned}
 D &= e^{r^2/4} (\Gamma/\nu) e^{-r^2/4} \\
 &= \nu^2 - \frac{1}{4} r^2 + \frac{3}{2}
 \end{aligned}
 \quad (7)$$

by scaling the Laplace parameter as $s = p/\nu$. Then we obtain the equation

$$[s - D + \frac{x}{z}(s - D)\frac{x}{z} + \frac{y}{z}(s - D)\frac{y}{z}] F(\vec{r}, s) = Q_0(r)
 \quad (8)$$

with

$$Q_0(r) = (2\pi)^{-3/2} e^{-r^2/4} = P_0(\vec{r}) e^{r^2/4}
 \quad (9)$$

Note that the operator $-D$ is the Hamiltonian operator of a three-dimensional harmonic oscillator.

In the static limit of $\nu = 0$, Eq. (5) gives

$$M_z(\vec{r}, p) = \frac{s + z^2}{s(s + r^2)} P_0(\vec{r})
 \quad (10)$$

By integrating over the variable \vec{r} and transforming back to the time domain, the relaxation function $G(t)$ is found to be

$$G(t) = \frac{1}{3} + \frac{2}{3}(1 - \Delta^2 t^2) e^{-\Delta^2 t^2/2}
 \quad (11)$$

which is the Kubo-Toyabe function with a minimum, $G = 0.1846$, at $t = \sqrt{3}/\Delta$.

On the otherhand, Eq. (8) gives the static limit

$$F(\vec{r}, s) = \frac{z^2}{s r^2} Q_0(r)
 \quad (12)$$

which yields the value $1/3$ for the relaxation function G irrespective of time t , which corresponds to the first term of the expression (11). For finite but small values of ν ($\ll \Delta$), the solution of Eq. (8) gives the decay of this part of the relaxation function. Hereafter we consider only this part. In this approximation, the parameter Δ is no longer present, so that time t is scaled by ν .

§3. A Variational Method

We write Eq. (8) as

$$A F = Q_0 \quad (13)$$

An inhomogeneous equation of this type is associated with the variation principle,

$$\frac{1}{2} (F, AF) - (F, Q_0) = \text{extremum} \quad (14)$$

where the bracket means an inner product of two functions defined as an integral over the space of \vec{r} . We assume the variation function of the form

$$F(\vec{r}, s) = (z^2/r^3) f(r) \quad (15)$$

where $f(r, s)$ is a function of $r = |\vec{r}|$. Inserting (15) into the right hand side of Eq. (8), we find

$$A F = -\frac{1}{r} (\Lambda - s) f(r) \quad (16)$$

where

$$\Lambda = -\frac{d^2}{dr^2} + w(r) \quad (17)$$

with

$$w(r) = \frac{3}{2} - \frac{r^2}{4} - \frac{4}{r^2}$$

We assume the boundary condition

$$f(0) = 0 \text{ and } f(\infty) = 0 \quad (18)$$

requiring that the integral of $M_2[f, \rho]$, Eq. (6), over \vec{r} is convergent.

Then Eq. (14) becomes

$$\int_0^\infty [f'^2 + (s - w)f^2] dr - \int_0^\infty Q_0(r) f(r) r dr = \text{extremum} \quad (19)$$

The Euler equation is

$$(\Lambda - s) f = -f_0 \quad (20)$$

where

$$f_0 = rQ_0(r) \quad (21)$$

or

$$f''(r) + \left(\frac{3}{2} - \frac{r^2}{4} - \frac{4}{r^2} - s\right)f(r) = -f_0(r) \quad (22)$$

which is Eq. (8) for the function $f(r, s)$ introduced by Eq. (15).

Now we choose the trial functions as

$$f_n(r) = f_0(r) \sum_{k=0}^n c_k r^k \quad (23)$$

The first term on the right hand side of Eq. (19) is quadratic in the parameters c_0, c_1, \dots , while the second term is linear. By the extremum condition we obtain a set of inhomogeneous linear equations for the parameters. This is solved numerically. With f and F thus determined, we integrate the function $M_{\frac{1}{2}}[\vec{r}, p]$, Eq. (6) over \vec{r} to obtain the Laplace transform $G[p]$ of the relaxation function $G(t)$, which is expanded in partial fractions,

$$G[p] = \sum_{j=0}^n b_j / (s + \gamma_j) \quad (24)$$

Then the relaxation function is obtained in the form

$$G(t) = \sum_{j=0}^n b_j e^{-\gamma_j t} \quad (25)$$

corresponding to the n -th trial function (23). The expansion coefficients and the corresponding relaxation rates thus calculated are listed in Table 1.

The crudest approximation gives a simple exponential decay with $\gamma_0 = 4 \nu$ as was calculated by Toyabe [2]. In better approximations, the slowest decay constant approaches the value 1.56155. This is considerably smaller than the crudest value. It is also conjectured from the Table that the decay constants are regularly spaced by 2, namely that

$$\gamma_n = (1.56155 + 2n) \nu \quad (26)$$

Table 1. Calculated coefficients and relaxation rates

n	b_j	γ_j
0	0.333333	4.000000
	0.2355278	1.562631
2	0.0760979	4.401605
	0.0217076	30.038927
	0.2361861	1.561582
	0.0470295	3.561571
4	0.0218435	5.637633
	0.0241911	11.45185
	0.0040832	97.18752
	0.2362125	1.561556
	0.0470335	3.561560
	0.0183609	5.561571
6	0.0097856	7.578202
	0.0111633	10.657820
	0.0095877	24.39665
	0.0011901	225.0364

Indeed this is proved analytically in the next section. The sixth approximation in the Table gave good results up to $n = 4$. Therefore the relaxation function which corresponds to the $1/3$ term in Eq. (11) may be expressed as

$$\begin{aligned}
 G(t) = & 0.23621 \exp(-1.5616 \nu t) + 0.04703 \exp(-3.56161 \nu t) \\
 & + 0.01836 \exp(-5.5616 \nu t) + \dots
 \end{aligned}
 \tag{27}$$

§ 4. An Exact Treatment

In this section an exact treatment is developed for Eq. (20). We consider the eigenvalue problem,

$$\Lambda u_n(r) = -\lambda_n u_n(r) \quad (28)$$

for which the boundary conditions are $u_n(0) = u_n(\infty) = 0$ and the eigenfunctions are quadratically integrable for $0 < r < \infty$. Obviously we have

$$(u_m, \Lambda u_n) = (u_n, \Lambda u_m)$$

and

$$(u_m, u_n) = \delta_{mn}$$

where an inner product is defined by

$$(f_1, f_2) = \int_0^\infty dr f_1(r) f_2(r) \quad (29)$$

Equation (20) is solved in the form,

$$f(r, s) = \sum_{n=0}^{\infty} \frac{1}{s + \lambda_n} (f_0, u_n) u_n(r) \quad (30)$$

Then the Laplace transform $G[p]$ of the relaxation function $G(t)$ is obtained with the use of (6), (15) and (21) as

$$\begin{aligned} G[p] &= \int M_z[\vec{r}, p] d\vec{r} \\ &= \int_0^\infty dr \frac{z^2}{r^3} f(r) e^{-r^2/4} \\ &= \frac{4}{3} (2\pi)^{3/2} \int_0^\infty f(r, s) f_0(r) dr \\ &= \frac{4}{3} (2\pi)^{3/2} \sum_{n=0}^{\infty} \frac{1}{s + \lambda_n} (f_0, u_n) (u_n, f_0) \end{aligned} \quad (31)$$

and the relaxation function $G(t)$ as

$$G(t) = \frac{4}{3} (2\pi)^{3/2} \sum_{n=0}^{\infty} \exp(-\lambda_n vt) |(f_0, u_n)|^2 \quad (32)$$

By the completeness of the eigenfunctions $\{u_n\}$, we see that

$$G(0) = \frac{4}{3} (2\pi)^{-3/2} (f_0, f_0) = \frac{1}{3} \quad (33)$$

Now we change the variables to

$$\rho = r^2/2 \quad \text{and} \quad f(r) \pm g(\rho) e^{-\rho/2} \quad (34)$$

The operator in Eq. (28) is transformed to

$$\begin{aligned} \Lambda_\rho &= \sqrt{2\rho} \frac{d}{d\rho} \sqrt{2\rho} \frac{d}{d\rho} + w(\rho) \\ &= 2\rho \frac{d^2}{d\rho^2} + \frac{d}{d\rho} + w(\rho) \end{aligned} \quad (35)$$

with

$$w(\rho) = \frac{3}{2} - \frac{\rho}{2} - \frac{2}{\rho} \quad (36)$$

Equation (28) is then transformed to

$$L v_n(\rho) = -\lambda_n v_n(\rho) \quad (37)$$

where

$$\begin{aligned} L &= e^{\rho/2} \Lambda_\rho e^{-\rho/2} \\ &= 2\rho \frac{d^2}{d\rho^2} + (1-2\rho) \frac{d}{d\rho} + (1-\frac{2}{\rho}) \end{aligned} \quad (38)$$

The eigenfunctions are orthogonal, namely

$$(v_m, v_n) = \int_0^\infty \frac{d\rho}{\sqrt{2\rho}} e^{-\rho} v_m(\rho) v_n(\rho) = \delta_{mn} \quad (39)$$

which is directly proved by Eq. (37).

Equation (37) is solved by the standard method assuming the solution

$$v_n = \sum_{k=0}^n a_{n,k} \rho^{\alpha+k} \quad (40)$$

for which the recurrence relation of the coefficients is

$$\frac{a_{n,k+1}}{a_{n,k}} = \frac{2\alpha + 2k - 1 - \lambda_n}{2\alpha^2 + (4k+3)\alpha + 2k^2 + 3k - 1}$$

The condition that $a_{n,-1} = 0$ gives

$$2\alpha^2 - \alpha - 2 = 0, \text{ or } \alpha = \frac{1}{4} (1 + \sqrt{17}) \quad (41)$$

The negative root of the quadratic equation is abandoned by the boundary condition at $r = 0$. The power series in (39) must be terminated at an integer n , because the solution will otherwise diverge at $\rho \rightarrow \infty$ as $\exp \rho$. Therefore, the eigenvalues are given by

$$\lambda_n = 2\alpha - 1 + 2n = 1.5615528 + 2n \quad (42)$$

The eigenfunctions are explicitly given by the polynomials

$$v_n(\rho) = N_n \sum_{k=0}^n (-)^k \frac{n!}{k! (n-k)!} \frac{\Gamma(2\alpha + \frac{1}{2}) \Gamma(\alpha+k+1)}{\Gamma(2\alpha + \frac{1}{2} + k)} \rho^k \quad (43)$$

where N_n is the normalization factor. With this we find

$$\begin{aligned} (f_0, u_n) &= (2\pi)^{-3/2} \int_0^\infty e^{-\rho} v_n(\rho) d\rho \\ &= (2\pi)^{-3/2} N_n \sum_{k=0}^n (-)^k \frac{n!}{k! (n-k)!} \\ &\quad \times \frac{\Gamma(2\alpha + 1/2) \Gamma(\alpha+k+1)}{\Gamma(2\alpha + 1/2 + k)} \end{aligned} \quad (44)$$

and

$$\begin{aligned} N_0^2 &= \sqrt{2}/\Gamma(2\alpha + \frac{1}{2}) \\ N_1^2 &= N_0^2 (2\alpha + \frac{1}{2}) \\ N_2^2 &= N_0^2 (2\alpha + \frac{1}{2}) (2\alpha + \frac{3}{2})/2 \end{aligned} \quad (45)$$

$$b_0 = \frac{2}{3\sqrt{\pi}} (\alpha+1)^2 / \Gamma(2\alpha + \frac{1}{2}) = 0.2362$$

$$b_1/b_0 = (\alpha - \frac{1}{2})^2 / (2\alpha + \frac{1}{2}), \quad (46)$$

$$b_2/b_1 = (\alpha + \frac{1}{2})^2 / [2(2\alpha + \frac{3}{2})].$$

These give excellent numerical agreement with the variational calculation (27). This is not trivial, since the variational functions (23) are quite different in the analytic properties from the exact functions (30). This suggests that the same variational calculation can be applied to more complex cases where an external magnetic field is present. Such calculations will be tried in another paper.

§ 5 Conclusion

We have examined the long time tail of the Kubo-Toyabe-function for the case where the Gaussian modulation is very slow in comparison to its magnitudes. Calculations here are limited to the zero-field relaxation. It consists generally of exponentially decaying functions. The slowest rate, which is the most important, is equal to 1.5616ν , where ν is the correlation rate of the Gaussian modulation. We first tried a variational formulation and then an exact treatment. The excellent agreement of the two treatments gives us hope that the variational method can be applied with sufficient accuracy to more complicated cases where finite magnetic fields are present. Direct simulations of spins modulated by a Gaussian random field were also made for the purpose to test the accuracy of the variational calculation. The result was satisfactory, but it is not reported here, since the accuracy of the variational calculation was proved by the agreement with the exact treatment, which we were not sure to be possible when we started this problem.

References

- 1) R. Kubo and T. Toyabe : Magnetic Resonance and Relaxation , Proceedings of the XIVth Colloque Ampere Ljubljana, 1966, ed. R. Blinc, North Holland 1967, pp 810-823.
- 2) T. Toyabe : Master thesis, Department of Physics, University of Tokyo, 1966.
- 3) R. S. Hayano, Y. J. Uemura, J. Imazato, N. Nishida, T. Yamazaki and R. Kubo : Phys. Rev. B 29 (1979) 850.
- 4) R. Kubo : Hyperfine Interactions 8 (1981) 731.

DISCLAIMER

This report was prepared as an account of work sponsored by an agency of the United States Government. Neither the United States Government nor any agency thereof, nor any of their employees, makes any warranty, express or implied, or assumes any legal liability or responsibility for the accuracy, completeness, or usefulness of any information, apparatus, product, or process disclosed, or represents that its use would not infringe privately owned rights. Reference herein to any specific commercial product, process, or service by trade name, trademark, manufacturer, or otherwise does not necessarily constitute or imply its endorsement, recommendation, or favoring by the United States Government or any agency thereof. The views and opinions of authors expressed herein do not necessarily state or reflect those of the United States Government or any agency thereof.

Determination of the Electronic Structure of Anomalous Muonium in GaAs from Nuclear Hyperfine Interactions

R. F. Kiefl¹, M. Celio¹, T. L. Estle², G. M. Luke³, S. R. Kreitzman³,
J. H. Brewer³, D. R. Noakes³, E. J. Ansaldo⁴, and K. Nishiyama⁵

¹TRIUMF, 4004 Wesbrook Mall, Vancouver, Canada V6T 2A3,

²Rice University, Houston, Texas 77251,

³University of British Columbia, Vancouver, Canada V6T 2A3,

⁴University of Saskatchewan, Saskatoon, Canada S7N 0W0,

⁵University of Tokyo, Tokyo 113, Japan

March 13, 1987

Abstract

Nuclear hyperfine structure of the anomalous muonium center (Mu^*) in GaAs has been resolved in muon spin rotation frequency spectra and studied in detail using level-crossing-resonance spectroscopy. A comparison of the measured hyperfine parameters with the free atom values indicates that 38% (45%) of the spin density is on one Ga (As) on the $\langle 111 \rangle$ symmetry axis of Mu^* with the ratio of p to s spin density equal to about 4 (23). These results support a recently proposed model in which Mu^* is a neutral interstitial located close to the center of a Ga-As bond.

PACS numbers: 71.55.Eq, 76.70.-r, 76.75.+i
to be published in Physical Review Letters

The electronic structure of a muonium defect center is expected to be identical to that of the analogous hydrogen center, except for vibrational effects arising because the positive muon has only 1/9th the mass of the proton. However, muonium defect centers are readily observed in semiconductors via the technique of muon spin rotation (μ SR) whereas the analogous hydrogen centers have not been observed using electron spin resonance (ESR). The spectra of muon spin precession frequencies have revealed the existence of two quite different paramagnetic centers, normal muonium (Mu) and anomalous muonium (Mu^*), in diamond [1], silicon [2,3], germanium [4], and most recently in GaAs and GaP [5]. Mu is characterized by a large isotropic muon hyperfine (μhf) interaction, whereas Mu^* has a small, highly anisotropic μhf interaction with trigonal symmetry.

Despite years of study, it is still not known what Mu^* is — i.e., where the muon is situated, what displacements of the neighboring atoms occur, and what the charge and the electronic state are. Measurements of the μhf interaction alone have not led to a clear picture of the defect. A much better understanding of Mu^* should result from measuring the nuclear hyperfine (nhf) interactions since they characterize the electron spin density in the region of the surrounding nuclear spins.

In this paper we report precise determination of nhf parameters for Mu^* in GaAs using a novel level-crossing-resonance (LCR) technique [6,7,8,9] and conventional μ SR. We conclude that the larger nhf interactions originate from the nearest neighbor (nn) Ga and As nuclei on the $\langle 111 \rangle$ symmetry axis of Mu^* . Comparison of the hf parameters with the free atom values indicates that 83% of the spin density is located on these two atoms, thus strongly supporting a recently proposed model [10,11] in which Mu^* is neutral interstitial muonium located close to the center of a Ga-As bond.

Following Abragam's suggestion for muon LCR experiments [6], studies of muonium-substituted free radicals [7,8,12] have demonstrated the utility of the method for simple isotropic systems. The LCR spectra for muonium defect centers in crystals are considerably more complicated as a result of anisotropy in the μhf and nhf tensors as well as the presence of neq interactions for nuclei with spin greater than $\frac{1}{2}$. The present LCR data can be described using a system consisting of an electron spin S , a muon spin I , and a

single nuclear spin \mathbf{J} . The spin Hamiltonian appropriate to Mu^* can be written:

$$\begin{aligned} \mathcal{H} = & g\mu_B \mathbf{H} \cdot \mathbf{S} - g_\mu \mu_\mu \mathbf{H} \cdot \mathbf{I} + A_{\parallel}^\mu S_z I_z + A_{\perp}^\mu (S_x I_x + S_y I_y) \\ & - g_n \mu_n \mathbf{H} \cdot \mathbf{J} + A_{\parallel}^n S_z J_z + A_{\perp}^n (S_x J_x + S_y J_y) + Q[3J_z^2 - J(J+1)] \end{aligned} \quad (1)$$

where \mathbf{H} is the magnetic field, $A_{\parallel}^{\mu(n)}$ and $A_{\perp}^{\mu(n)}$ are the parallel and perpendicular μhf (nhf) parameters respectively, and Q is the neq parameter. We have assumed that the μhf , nhf and neq tensors are all axially symmetric about a common axis \hat{z} , which is one of the crystalline (111) axes, and that the g -tensors are isotropic. For each of the electron spin states, one may derive an approximate effective muon-nuclear spin Hamiltonian, which is valid for high fields and small Q :

$$\mathcal{H}_{eff} = -g_\mu \mu_\mu \mathbf{H}^\mu \cdot \mathbf{I} - g_n \mu_n \mathbf{H}^n \cdot \mathbf{J} + \frac{1}{2} Q [3(\hat{z} \cdot \hat{n})^2 - 1] [3J_n^2 - J(J+1)] \quad (2)$$

where J_n is the component of \mathbf{J} along \hat{n} , the unit vector in the direction of \mathbf{H}^n . The components of the effective fields \mathbf{H}^i parallel and normal to \mathbf{H} are respectively

$$\begin{aligned} H_{\parallel}^i &= H \mp (A_{\perp}^i \sin^2 \theta + A_{\parallel}^i \cos^2 \theta) / (2g_i \mu_i) \\ H_{\perp}^i &= \mp (A_{\perp}^i - A_{\parallel}^i) \sin 2\theta / (4g_i \mu_i) \end{aligned} \quad (3)$$

where i equals μ or n , θ is the angle between \hat{z} and \mathbf{H} , and the upper (lower) sign is for M_S positive (negative). The frequencies of the magnetic-dipole transitions for the muon and nuclear spins are given by

$$h\nu_\mu (M_I \leftrightarrow M_I - 1) = g_\mu \mu_\mu H^\mu \quad (4)$$

$$h\nu_n (M_J \leftrightarrow M_J - 1) = g_n \mu_n H^n - \frac{3}{2} Q [3(\hat{z} \cdot \hat{n})^2 - 1] (2M_J - 1) \quad (5)$$

where M_I (M_J) is the magnetic quantum number for quantization along \mathbf{H}^μ (\mathbf{H}^n). Note that for each value of M_S there is one possible value for ν_μ and $2J$ values for ν_n . The most prominent LCRs occur at applied fields where the muon transition frequency (Eq. 4) equals one of the nuclear transition frequencies (Eq. 5) [7,8,12], the same condition as for muon-nuclear cross relaxation.

This experiment was carried out at TRIUMF on the M15 beamline, using low-momentum (28.6 MeV/c) positive muons that were highly polarized (>95%), either parallel or perpendicular to their momenta. The muons were stopped in a single crystal wafer of high

resistivity (8×10^7 ohm-cm) GaAs supplied by Cominco Ltd., Trail, B.C., Canada. It was maintained at 10 K with one of the primary crystal orientations ($\langle 100 \rangle$, $\langle 111 \rangle$, or $\langle 110 \rangle$) along \mathbf{H} . The μ SR frequency spectra in a transverse magnetic field of 1.2T, where the muon spin is decoupled from all nuclear spins [13], were in good agreement with the μhf parameters for Mu^* reported previously [5] (see Table I), with a typical crystal misalignment of 1° . The LCRs were detected as a reduction in the time-integrated muon decay asymmetry along \mathbf{H} , the direction of the initial muon polarization [7]. A square wave modulation field of ± 5 mT was applied, causing the LCRs to appear to be differentiated in the resulting asymmetry difference spectra (see Fig. 1).

Part of the LCR spectrum for Mu^* in GaAs with \mathbf{H} parallel to the $\langle 100 \rangle$ direction is shown in Fig. 1a. It is particularly simple because for this orientation the four possible Mu^* centers, corresponding to the four $\langle 111 \rangle$ symmetry axes, are all equivalent ($\theta = 54.7^\circ$) and therefore there are fewer LCRs. Also, for \mathbf{H} along a $\langle 100 \rangle$ direction H_{\perp}^{μ} is large (see Eq. 3) and thus ν_{μ} has an appreciable minimum value. Consequently, there are no level crossings with nuclei which have hf couplings less than about 70 MHz, as there can be for $\theta = 0^\circ$ or 90° . The six prominent LCRs in Fig. 1a are all attributed to one ^{75}As nucleus (spin $\frac{3}{2}$ and 100% abundant) on the $\langle 111 \rangle$ symmetry axis of Mu^* . Each value of M_S gives rise to three resonances which are split by the neq interaction and small off diagonal terms in \mathcal{H}_{eff} (not shown in Eq. 2). The ^{75}As nhf and neq parameters given in Table I were obtained by fitting the positions of all the observed LCRs to those predicted from an exact diagonalization of Eq. 1.

For the $\langle 110 \rangle$ orientation the crystal was aligned so that there were no measurable splittings in the muon precessional frequencies associated with the $\theta = 35.3^\circ$ centers. Eight LCRs were observed between 3.0 and 3.3 T (see Fig. 1b), all attributed to one ^{69}Ga nucleus (spin $\frac{3}{2}$ and an isotopic abundance of 60.4%) on the Mu^* symmetry axis. Six correspond to centers where $\theta = 90^\circ$ and two to those with $\theta = 35.3^\circ$, as indicated in Fig. 1b. Four additional ^{69}Ga LCRs and the twelve ^{71}Ga LCRs are predicted to occur in higher fields beyond the limit of our magnet. However, they are not needed to obtain the hf and neq parameters which are given in Table I.

Effects of nhf interactions were also observed in the frequency spectra in transverse

magnetic fields between 0.3 and 0.5 T (see Fig. 2a for a $\langle 110 \rangle$ spectrum). In such intermediate fields, the muon is selectively coupled to the nuclei with the larger hf parameters [14], giving rise to the observed structure. Theoretical spectra (e.g., Fig. 2b) were obtained by exact diagonalization of the spin Hamiltonian using the parameters in Table I and including both gallium isotopes. From the striking similarity of the experimental and theoretical spectra, we may conclude that there are no other nuclei with comparable or larger hf parameters and that our assignment of the LCRs is correct.

Many other LCRs were observed in the $\langle 111 \rangle$ and $\langle 110 \rangle$ spectra in the magnetic field range 0.3 – 0.8 T, where one expects LCRs from nhf parameters less than about 100 MHz. These smaller nhf couplings will be described in a later publication.

Comparison of the measured hf parameters to valence s and p atomic orbital values [15] gives estimates of the contribution of these atomic orbitals to the defect molecular orbital of the unpaired electron [16]. In this way we obtain a total spin density on the As (Ga) of 45% (38%) with the p to s density ratio 23 (4) (see Table I). The large spin densities on both atoms and the appreciable distance between two like atoms along the $\langle 111 \rangle$ axis imply that the Ga and As are nn nuclei on this axis. Furthermore, the magnitude of the anisotropic μhf interaction, which is about 1.5 times that from a $2p$ orbital, demonstrates that the μ^+ is within a few atomic radii of this Ga-As pair.

The present results strongly support a recently proposed model [10,11] in which Mu^* is a neutral interstitial located near the center of a Ga-As bond. This model predicts that most of the unpaired spin density is located on the two nn nuclei on the $\langle 111 \rangle$ symmetry axis and that the muon is near a node in the spin density, all in agreement with the present results. For the bond-centered site to be a minimum in the total energy, there should be an increase in the Ga-As spacing, as has been predicted theoretically for Mu^* in diamond and silicon [10,11]. From the measured ratios of p to s spin densities, assuming orthogonal s - p hybridized atomic valence orbitals directed along the internuclear axes, fixed next nn , and estimating s -orbital spin polarization from theoretical calculations on the GeH_3 radical [17], we estimate that the nn As and Ga are displaced 0.65(17) Å and 0.14(6) Å away from the bond center respectively. (The uncertainties arise from spin polarization effects which are not known accurately.) These displacements imply an increase in the Ga-As bond length

of about 32(7)%.

Our results cannot be explained by any other model proposed for Mu^* in semiconductors. In the vacancy associated model [18] the unpaired spin would be primarily on the nn As (Ga) if the muon is in a Ga (As) vacancy. The distance to the closest Ga (As) on the symmetry axis is so great that no significant spin density is expected there. In the hexagonal site model [19] one would expect the spin density to be primarily on the six nn nuclei off the symmetry axis. In the back bonding model [20] there is no reasonable explanation for the almost equal spin densities on the two nn nuclei on the $\langle 111 \rangle$ axis and the small s spin density on the muon.

In conclusion, we have obtained detailed information on the electronic structure of Mu^* in GaAs, having used EPR spectroscopy to determine unambiguous and accurate values of all the larger hyperfine parameters. We find that most of the electron spin density is on the nearest neighbor Ga and As on the $\langle 111 \rangle$ symmetry axis. The atomic characters are considerably more p -like than sp^3 , thus implying large lattice relaxation. These results strongly support the bond centered interstitial model for Mu^* in semiconductors and virtually rule out all other models proposed to date.

This work was supported by the National Research and Natural Sciences and Engineering Research Councils of Canada. One of us (T.L.E.) would like to acknowledge support from the U.S. National Science Foundation grant DMR 79-09223 and Robert A. Welch Foundation grant C-1048. We would like to thank J.-M. Spaeth for helpful suggestions.

References

- [1] E. Holzschuh, W. Kündig, P.F. Meier, B.D. Patterson, J.P.F. Sellschop, M.C. Stemmet, and H. Appel, *Phys. Rev. A* **25**, 1272 (1982).
- [2] J.H. Brewer, K.M. Crowe, F.N. Gygax, R.F. Johnson, B.D. Patterson, D.G. Fleming, and A. Schenck, *Phys. Rev. Lett.* **31**, 143 (1973).
- [3] B.D. Patterson, A. Hinterman, W. Kündig, P.F. Meier, F. Waldner, H. Graf, E. Recknagel, A. Weidinger, and Th. Wichert, *Phys. Rev. Lett.* **40**, 1347 (1978).
- [4] E. Holzschuh, H. Graf, E. Recknagel, A. Weidinger, and Th. Wichert, *Phys. Rev. B* **20**, 4391 (1979).
- [5] R.F. Kiefl, J.W. Schneider, H. Keller, W. Kündig, W. Odermatt, B.D. Patterson, K.W. Blazey, T.L. Estle, and S.L. Rudaz, *Phys. Rev. B* **32**, 530 (1985).
- [6] A. Abragam, *C.R. Acad. Sci. (Paris), Ser. 2*, **299**, 95 (1984).
- [7] R.F. Kiefl, S.R. Kreitzman, M. Celio, R. Keitel, G.M. Luke, J.H. Brewer, D.R. Noakes, P.W. Percival, T. Matsuzaki, and K. Nishiyama, *Phys. Rev. A* **34**, 681 (1986).
- [8] M. Heming, E. Roduner, B.D. Patterson, W. Odermatt, J. Schneider, Fp. Baumeler, H. Keller, and M. Savic, *Chem. Phys. Lett.* **128**, 100 (1986).
- [9] R.F. Kiefl, *Hyp. Int.* **32**, 707 (1986).
- [10] S.F.J. Cox and M.C.R. Symons, *Chem. Phys. Lett.* **126**, 516 (1986); T.A. Claxton, A. Evans, and M.C.R. Symons, *J. Chem. Soc., Faraday Trans. 2*, **82**, 2031 (1986).
- [11] T.L. Estle, S. Estreicher, and D.S. Marynick, *Hyp. Int.* **32**, 637 (1986); *Phys. Rev. Lett.*, submitted (MS. LZ3269).
- [12] P.W. Percival, R.F. Kiefl, S.R. Kreitzman, D.M. Garner, S.F.J. Cox, G.M. Luke, J.H. Brewer, K. Nishiyama, and K. Venkateswaren, *Chem. Phys. Lett.*, in press.
- [13] R.F. Kiefl, E. Holzschuh, H. Keller, W. Kündig, P.F. Meier, B.D. Patterson, J.W. Schneider, K.W. Blazey, S.L. Rudaz, and A.B. Denison, *Phys. Rev. Lett.* **53**, 90 (1984).
- [14] E. Roduner and H. Fischer, *Chem. Phys.* **54**, 261 (1981).
- [15] J.R. Morton and K.F. Preston, *J. Magn. Reson.* **30**, 577 (1978).
- [16] U. Kaufmann and J. Schneider. *Festkörperprobleme (Advances in Solid State Physics)*, Vol. XX, J. Treusch (ed.), p. 87 (Vieweg, Braunschweig, 1980).
- [17] K. Ohta, H. Nakatsuji, I. Maeda, and T. Yonezawa, *Chem. Phys.* **67**, 49 (1982).
- [18] N. Sahoo, K.C. Mishra, and T.P. Das, *Phys. Rev. Lett.* **55**, 1506 (1985).
- [19] T.L. Estle, *Hyp. Int.* **8**, 365 (1981).
- [20] B.D. Patterson, *Hyp. Int.* **17-19**, 517 (1984).

Tables

Table 1: The measured hyperfine and nuclear electric quadrupole parameters for Mu^* in GaAs and the inferred s and p atomic spin densities. The s and p spin densities are calculated from $\eta^2\alpha^2 = \frac{1}{3}(A_{||}^i + 2A_{\perp}^i)/A_p^{free}$ and $\eta^2\beta^2 = \frac{1}{3}(A_{||}^i - A_{\perp}^i)/A_p^{free}$ respectively, where the free atom values for s and p valence orbitals are obtained from [15]. All measured parameters have the same sign.

Nucleus	$A_{ }^i/h$ (MHz)	A_{\perp}^i/h (MHz)	Q/h (MHz)	$\eta^2\alpha^2$	$\eta^2\beta^2$
μ^+	218.54(3)	87.87(5)	—	0.0294	—
^{75}As	563.1(4)	128.4(2)	6.26(7)	0.0186	0.434
^{69}Ga	1052(2)	867.9(3)	0.36(1)	0.0761	0.301

Figures

Figure 1 The level-crossing-resonance spectra of Mu^* in GaAs for H applied along the (a) $\langle 100 \rangle$ and (b) $\langle 110 \rangle$ directions. The resonances are labeled by the nucleus involved, the sign of M_S , and θ , the angle between the symmetry axis and the magnetic field.

Figure 2 (a) Resolved nuclear hyperfine structure in the spectrum of muon precessional frequencies for Mu^* with $\theta = 90^\circ$, $M_S = -\frac{1}{2}$, and the magnetic field (0.30 T) applied parallel to $\langle 110 \rangle$. (b) The corresponding theoretical frequency spectrum using the parameters in Table I.

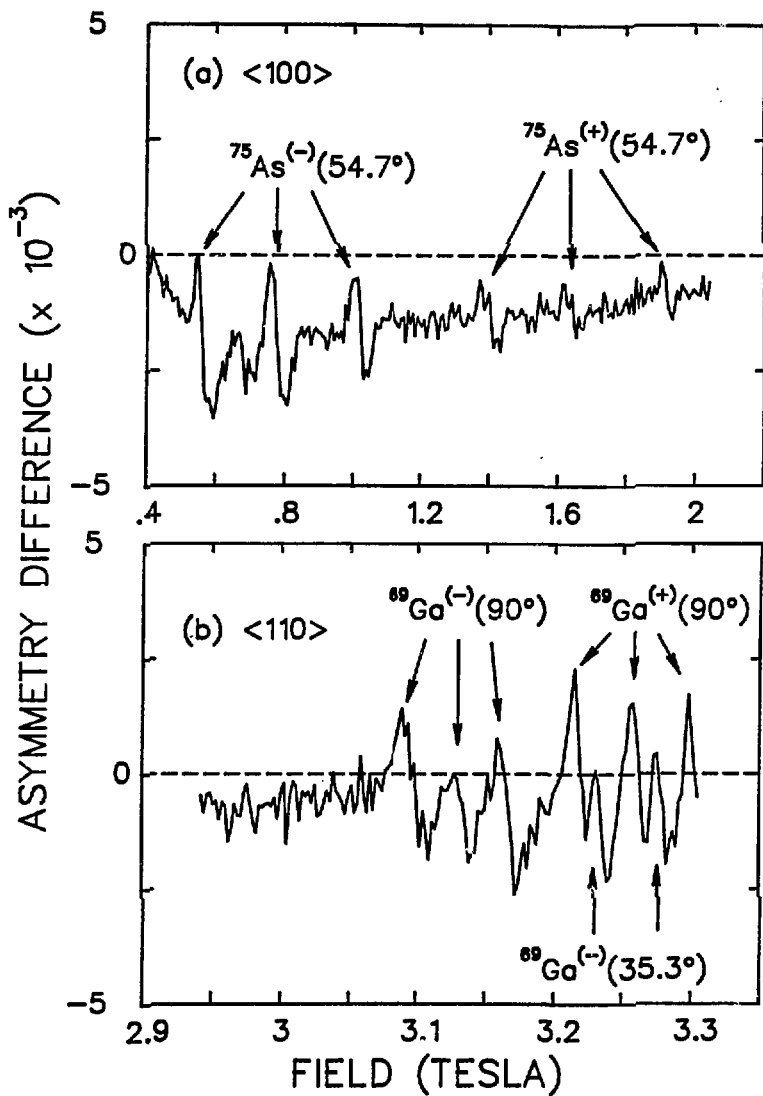


Fig. 1

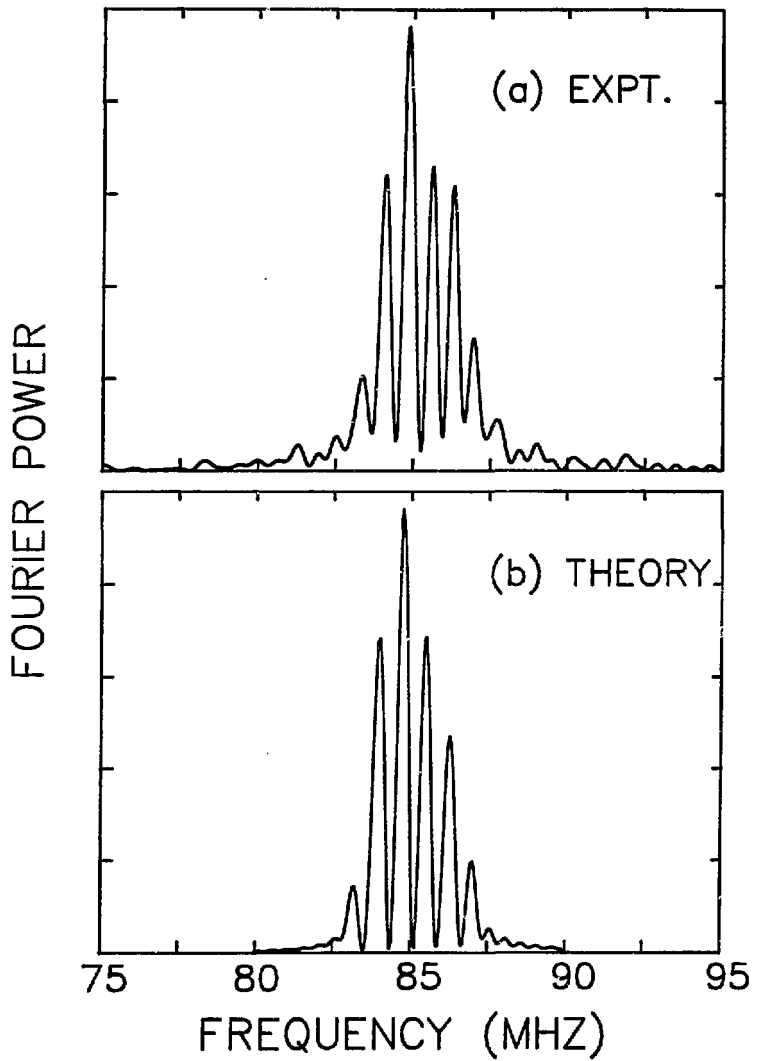


Fig. 2

ZERO FIELD μ^+ SPIN RELAXATION
IN $\text{Cd}_{1-x}\text{Mn}_x\text{Te}$ DILUTED MAGNETIC SEMICONDUCTORS

E.J. Ansaldo,* D.R. Noakes,** R. Keitel, S.R. Kreitzman**
J.H. Brewer,** and J.K. Furdyna***

TRIUMF

4004 Wesbrook Mall, Vancouver, B.C., Canada V6T 2A3

Abstract

Zero field μSR measurements were carried out on samples of the typical diluted magnetic semiconductor $\text{Cd}_{1-x}\text{Mn}_x\text{Te}$ as a function of composition in the range $0.27 \lesssim x \lesssim 0.65$, at temperatures in both the paramagnetic and the "spin glass" regions of the magnetic phase diagram. The results show the onset of complex diffusion-trapping behaviour at temperatures $T \gtrsim 60$ K for all concentrations. Below ~ 50 K the exponential relaxation found for the main signal is consistent with the interactions of the muon spin with rapidly fluctuating and rather large local hyperfine fields in these concentrated random diluted magnetic systems. In spite of the loss of signal near and below the transition temperature, the present results show that rapid spin fluctuations persist below T_g .

Diluted magnetic semiconductors (DMS) are semiconducting alloys in which magnetic ions are substituted for a fraction of the original atoms in the crystal. Most extensively studied are the II-VI compounds where a fraction x ($0 < x < 1$) of the group II cations are replaced by Mn^{2+} ions, as for example the $Cd_{1-x}Mn_xTe$ system, object of our initial μ SR investigations. While remaining wide gap semiconductors, such systems display unique electronic, magneto-optical [1], and, of primary importance here, macroscopic magnetic properties that are as yet not fully understood [1,2]. The spinglass-like cusp and remanence behaviour observed in the magnetic susceptibility for $x > 0.17$ has been rationalized in terms of a lattice frustration mechanism on the predominantly antiferromagnetic exchange interactions between the magnetic ions [2,3]. Recently, a thorough analysis of the high temperature region for all the DMS as randomly diluted Heisenberg antiferromagnets has shown that the Mn-Mn interaction originates in superexchange via the valence p-orbitals of the host anions [4]. For $CdMnTe$, at concentrations $x > 0.6$ no cusp was observed, and the magnetic susceptibility versus temperature curve hints at antiferromagnetic (AF) ordering. The magnetic scattering peaks also correspond to an AF structure, but no long-range order has been detected in neutron scattering experiments [5,6]. For $x=0.65$ the data are indicative of the formation of small (magnetic, not chemical) AF clusters with a T-dependent correlation length that saturates (at about 160 Å) at $T=30$ K, which is close to the transition temperature in the susceptibility [7].

Some information on the dynamics of the Mn spin system has been obtained in extensive electron paramagnetic resonance (EPR) studies [8-10]. Briefly, the EPR line broadens with increasing x and lowering

temperature, becoming too broad for measurement with conventional techniques close to the cusp temperature (T_g). A novel Faraday rotation technique [11] has been used to follow the broadening and shift of the EPR line to temperatures close to T_g . These results were phenomenologically interpreted in terms of random internal fields, with a Lorentzian distribution, and whose fluctuations are averaged over an unspecified characteristic time for the system [9,10].

In order to further investigate the question of the internal fields and their dynamics in the DMS we have initiated a series of zero field (ZF) and longitudinal field (LF) muon spin relaxation (μ SR) measurements on the CdMnTe system. The ZF- μ SR technique and its usefulness in the study of spin dynamics is well documented [12,13] (in particular, see ref. [12] where the instrumental and data analysis procedures used in previous spinglass studies in our laboratory are discussed in detail). Single crystalline samples of $\text{Cd}_{1-x}\text{Mn}_x\text{Te}$ with nominal concentrations $0.275 < x < 0.65$, grown by the Bridgman technique, were available from previous experiments at Purdue University [1,9,11]. Such samples have a homogeneous zincblende crystal structure, with the Mn ions occupying an fcc sublattice as they randomly substitute for Cd ions. The experiments were carried out at the M15 and M20 surface muons beam lines of TRIUMF tuned to the longitudinal polarization mode [14]. The samples were placed either in a gas-flow cryostat (3.5 to 300 K, ZF and small LF) or in a continuous-flow cold-finger cryostat (6 to 300 K, LF up to 4 kOe). Transverse field (TF) measurements were also carried out at low fields (< 0.02 T Oe) mostly for calibration purposes. Standard μ SR procedures were followed to extract the muon spin relaxation functions from the experimental data, and special attention was paid to the proper

determination of baselines [i.e., the zero-line of the ZF relaxation function $G_z(t)$], since this is of importance in assessing the existence of static components of the local field [12]. The TF calibrations were carried out separately from the ZF runs, to avoid possible remanence effects.

The muon spin relaxation functions in the paramagnetic state for all the samples were comparatively simple, consisting of a fast relaxing signal superimposed on a slowly relaxing "background" signal. This background signal was primarily due to a fraction of muons (10 to 15% of incident muons) stopping in the metal foils to which the crystal slices were attached to insure good thermal contact [15]. This was verified by using both Cu and Ag backings which yielded different relaxation functions for the background, as expected. The main signal could be fitted very well by a single exponential in all cases ($T \lesssim 200$ K). As shown in fig. 1 the relaxation rate, $\lambda(T)$, increases from a minimum of ca $5 \mu\text{s}^{-1}$ at $T-T_g \gtrsim 60$ K to values above the instrumental resolution ($\sim 200 \mu\text{s}^{-1}$) as a "transition" temperature T_g is approached. The T_g 's used in fig. 1 to show the divergent behaviour of $\lambda(T)$ are, within 2 K, the same as the cusp T_g in the "spin-glass" cases (i.e. $x < 0.6$) and the transition temperature (30 K) for the "AF" case ($x=0.65$). These results are consistent with large and rapidly fluctuating effective local fields on the muons due to their random environment of relatively large ($4.92 \mu_B$) atomic magnetic moments on the Mn^{2+} ions. The "high temperature" plateau apparent in the data of fig. 1 would then correspond to the exchange narrowing effect in NMR linewidths [16]. Assuming that the exchange fluctuation rate for the muons is the same as for the Mn^{2+} ions (muon spin system driven by the atomic moments), given in turn by the known exchange

energy (Jnn of ca. 8 K) [4], the strength of the local field at the μ^+ is too large to originate only in the dipolar interaction between Mn^{2+} ions and interstitial μ^+ in the lattice. Thus we surmise that the $Mn-\mu^+$ interaction has a hyperfine component due to the electronic spin-density mediating the Mn-Mn superexchange.

The behaviour of $\lambda(T)$ near and below T_g is typical of the slowing down effects on approaching an ordered state (dynamical depolarization in the spin-glass state [12]). The onset of quasi-static fields below the transition temperature normally results in a reduction of the experimental initial asymmetry, as observed in CdMnTe. In the present case however the asymmetry does not show the 1/3 recovery expected for the static fields in the ordered state [13] (spin-freezing in the spinglass cases). Furthermore, no change in the relaxation function was observed for $x=0.4$ and 0.65 either above or below T_g when a LF of 0.38 T was applied.

Similar behaviour obtains for the diluted spin-glass such as CuMn⁽¹²⁾, AgMn, and PdMn⁽¹⁷⁾ where the relaxation mechanism is still effective in a 0.5 T applied field and the spin fluctuations remain rapid below T_g , resulting in dynamic depolarization of the 1/3 component. In the present concentrated CdMnTe system the relaxation rates (fig. 1) are an order of magnitude higher, resulting in the drastic reduction of the experimental asymmetry (spectrometer dead-time ~20 ns) mentioned above and in the caption to fig. 1. Therefore it is not possible to clearly separate dynamical effects from inhomogeneous broadening in large random fields below T_g .

The "high-temperature" behaviour of $\lambda(T)$ is somewhat obscured by the onset of μ^+ diffusion (and possibly trapping) effects, apparent in the

data of fig. 1 at $T-T_g \gtrsim 60$ K. Such effects are seen more clearly in the data of fig. 2 for an $x=0.05$ sample doped with 10^{19} Cu atoms/cm³. That sample was prepared for purposes other than the present experiment, and the data of fig. 2 are shown only to illustrate qualitatively the effect of μ^+ motion in the lattice. In addition to the fast-relaxing component (due to the Mn^{2+} ions), a sizable fraction of the μ^+ display a relaxation function typical for a quasi-static interaction with nuclear dipoles, which is due predominantly to the Cu nuclei in this sample in addition to the sample holder background mentioned above. The long-time relaxation function (using the data for $t \gtrsim 100$ ns) changes noticeably above ca. 70 K (changes which can be seen by eye in fig. 2). Fitting that component of the relaxation function to a dynamic Kubo-Toyabe approximation yields a "hop-rate" of ca. $10 \mu s^{-1}$ for the muons at 100 K. It is interesting to note that the static shape reappears above ca. 150 K, which may indicate trapping in the lattice effects which need to be considered and studied further when applying the μ SR technique to the DMS dynamical behaviour in the high temperature limit.

ACKNOWLEDGEMENT

We are indebted to L. Asch and G.M. Kalvius for direct help and useful comments during the experimental runs. This research was supported by the NSERC of Canada and the NSF of the USA (J.K.F.).

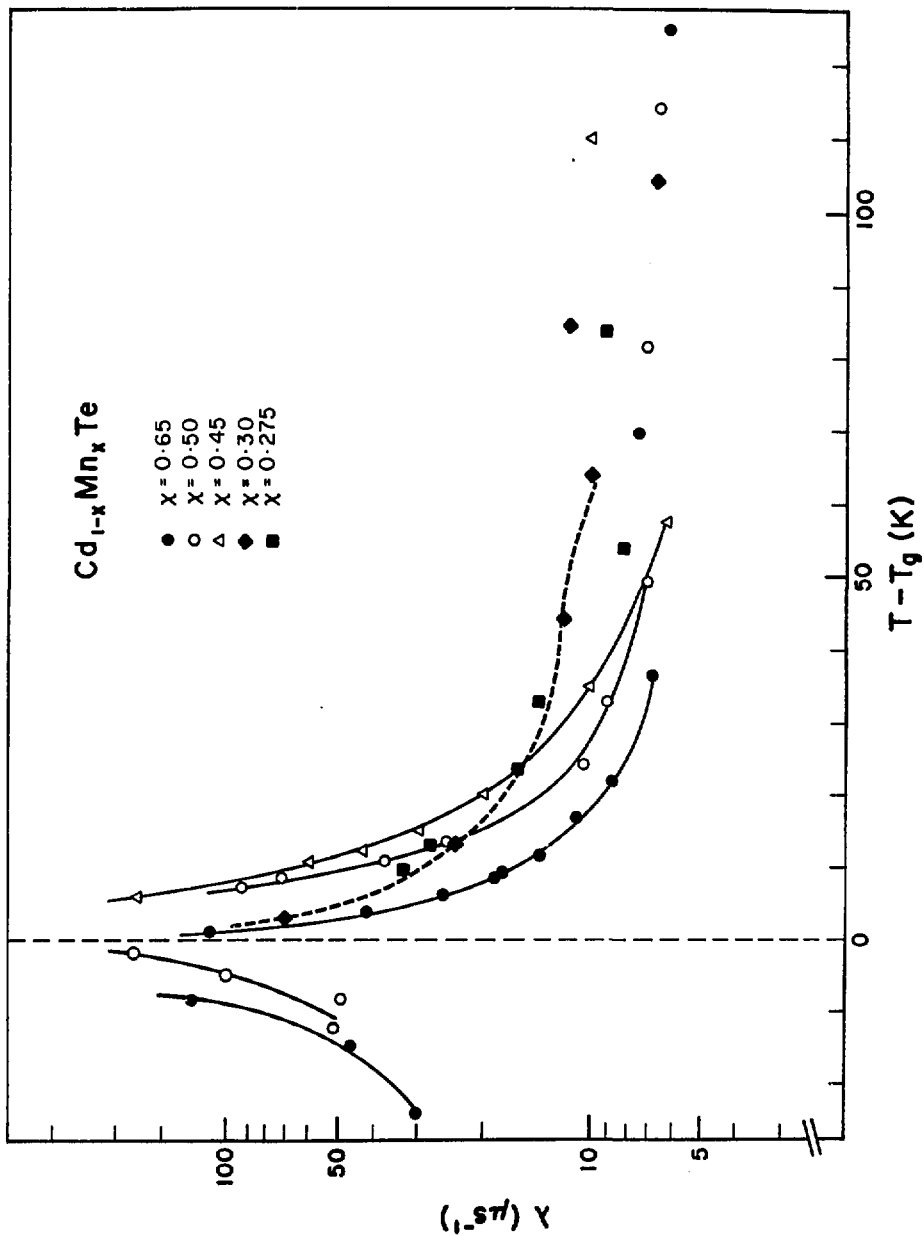
REFERENCES

- *Department of Physics, University of Saskatchewan, Saskatoon,
Saskatchewan, Canada S7N 0W0. Address for correspondence.
- **Department of Physics, University of British Columbia.
- ***Department of Physics, Purdue University, West Lafayette, IN 47907.
- [1] J.K. Furdyna, J. Appl. Phys. 53 (1982) 7637, and references therein.
- [2] R.R. Galazka, S. Nagata, and P.H. Keesum, Phys. Rev. B22 (1980) 3344.
- [3] L. DeSeeze, J. Phys. 10 (1977) 1353.
- [4] J. Spalek, A. Lewicki, Z. Tarnawski, J.K. Furdyna, R.R. Galazka, and F. Obuszko, Phys. Rev. B33 (1986) 3407.
- [5] G. Dolling, T.M. Holden, V.F. Sears, J.K. Furdyna, and W. Giriat, J. Appl. Phys. 53 (1982) 7644.
- [6] T. Giebultowicz, B. Lebeck, B. Buras, W. Minor, H. Kepa, and R.R. Galazka, J. Appl. Phys. 55 (1984) 2305.
- [7] U. Steingenberger, B. Lebeck, and R.R. Galazka, J. Magn. Mag. Mat. 54-57 (1986) 1285.
- [8] S.B. Oseroff, Phys. Rev. B25 (1982) 6584.
- [9] D.J. Webb, S.M. Bhagat and J.K. Furdyna, J. Appl. Phys. 55 (1984) 2310, and references therein.
- [10] H.A. Sayad and S.M. Bhagat, Phys. Rev. B31 (1985) 591.
- [11] R.E. Kremmer and J.K. Furdyna, J. Magn. Mag. Mat. 40 (1983) 185; Phys. Rev. B31 (1985) 1;
- [12] Y.J. Uemura, T. Yamazaki, D.R. Harshman, M. Senba, and E.J. Ansaldo, Phys. Rev. B31 (1985) 546 and references therein.
- [13] A. Schenk, "Muon Spin Rotation Spectroscopy - Principles and Applications to Solid State Physics" (Adam Hilger Ltd., Bristol, 1985).

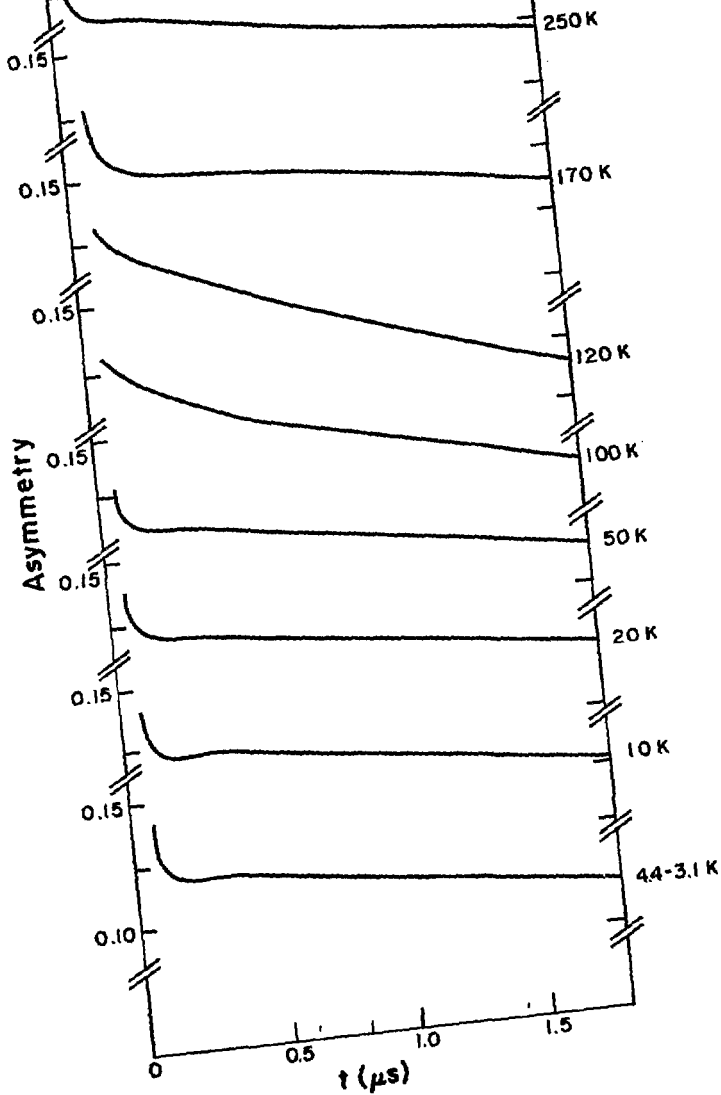
- [14] J.L. Beveridge, J. Doornbos, D. Garner, D. Arseneau, I.D. Reid, and M. Senba, Nucl. Instrum. Methods A240 (1985) 316.
- [15] In addition, the initial asymmetry (polarization at $t=0$) showed a "lost fraction" of ca. 20%, which indicates that a fraction of the μ^+ forms Muonium in the DMS [13].
- [16] V. Jaccarino, in Magnetism G.T. Rado and H. Suhl, Eds. (Academic Press, 1965) Vol. IIA, p.307.
- [17] R.H. Heffner, M. Leon, M. Schillaci, S.A. Dodds, G.A. Gist, D.E. MacLaughlin, J.A. Mydosh, and G.J. Nicuwenhuys, J. App. Phys. 55 (1984) 1703.

FIGURE CAPTIONS

1. Zero field relaxation rate of the main muon signal for the CdMnTe samples indicated. Below $T - T_g = 0$ the effective asymmetry of the signal is low (below ~ 0.04) and the relaxation rates shown have large errors, of the order of 40% (not displayed as error bars for clarity of the diagram). T_g denotes the transition temperature associated with a "spinglass" transition for $x \lesssim 0.6$ and an "antiferromagnetic" transition for $x=0.65$. The lines through the experimental points are drawn to guide the eye.
2. Relaxation functions obtained for the Cu-doped, $x=0.05$ sample. The solid lines are the result of two-signal fits to the data (not shown for clarity), consisting of an exponential (front end, typically $\lambda \approx 50 \mu\text{s}^{-1}$) and a dynamic Kubo-Toyabe components. The main purpose of the figure is to show the changes occurring at $50 \lesssim T \lesssim 150$ K. Below 50 K the KT component (presumably due to the impurity nuclear dipoles) is static, but changes rather abruptly to a dynamic case above 50 K, becoming quasi-static again at higher temperatures.



1863

 $\text{Cd}_{0.95}\text{Mn}_{0.05}\text{Te} (1 \times 10^{19} \text{Cu/cm}^3) \text{ZF}$ 

**Magnetic Penetration Depth and Flux-Pinning
Effects in High- T_c Superconductor $\text{La}_{1.85}\text{Sr}_{0.15}\text{CuO}_4$**

G. Aepli⁽¹⁾, *E. J. Ansaldo*⁽²⁾, *J. H. Brewer*⁽⁴⁾
R. J. Cava⁽¹⁾, *R. F. Kiefl*^(3,4), *S. R. Kreitzman*⁽⁴⁾,
G. M. Luke⁽⁴⁾, and *D. R. Noakes*⁽⁴⁾

February 12, 1987

ABSTRACT

We have performed muon spin relaxation (μSR) measurements on $\text{La}_{1.85}\text{Sr}_{0.15}\text{CuO}_4$ above and below its superconducting transition temperature, $T_c = 37\text{K}$. From transverse field μSR at 6K, the magnetic penetration depth is $\lambda \approx 2500\text{\AA}$, which, together with previous thermodynamic data and the London formula, implies a carrier density of $0.3 \times 10^{22} \text{ cm}^{-3}$. The temperature dependence of λ in our sintered powder sample differs from that for an ordinary homogenous superconductor. We also show that the longitudinal and transverse field μSR techniques are sensitive probes of H_{c1} and flux pinning effects.

(1) AT&T Bell Laboratories, Murray Hill, N. J. 07974.

(2) University of Saskatchewan, Saskatoon, Canada S7N 0W0

(3) TRIUMF and (4) University of B.C., Vancouver, Canada V6T 2A3

Compounds of the form $M_{2-x}Z_xCuO_4$ ($M = La^{(1-4)}$ or $Y^{(5)}$ and $Z = Ba^{(1,5)}$, $Sr^{(2-4)}$ or $Ca^{(2)}$) are superconductors with unprecedentedly high transition temperatures. For example, for $M = La$, $Z = Sr$ and $x = 0.15$, the bulk T_c is 37K, and correspondingly, the upper critical field H_{c2} exceeds 220kG. In the present paper, we describe experiments in which positive muons are used as microscopic probes of the internal fields in $La_{1.85}Sr_{0.15}CuO_4$ below T_c . Muon spin relaxation (μ SR) is especially suited to measuring quantities such as the magnetic penetration depth (λ) because it does not require special-purpose samples, such as thin films or spheres of controlled dimensions.⁽⁵⁾

We performed our μ SR measurements at the M15 surface muon channel of TRIUMF. The sample, a sintered polycrystalline pellet, 1 cm in diameter and 2mm thick, was prepared by means described elsewhere⁽³⁾ and mounted perpendicular to the incident beam. In time differential μ SR experiments, muons are stopped one at a time in the sample, where they decay, emitting positrons preferentially along their final polarization.⁽⁷⁾ Data are collected as a function of time t after arrival of the individual muons in the sample by counting the numbers $N_+(t)$ and $N_-(t)$ of positrons emitted in the directions parallel and antiparallel to the incident muon spin. The resulting ratio, $(N_+(t) - N_-(t))/(N_+(t) + N_-(t))$, is proportional to the time-dependent polarization of the muon ensemble.⁽⁸⁾ A magnetic field can be applied either parallel (longitudinal) or perpendicular (transverse) to the initial muon polarization, yielding respectively a " T_1 "-type relaxation function $G_{zz}(t)$ or a " T_2 "-like relaxation envelope $G_{xx}(t)$ modulating a precessing muon decay

asymmetry, just as for free induction decay in NMR.⁽⁷⁾

Fig. 1 shows the TF- μ SR precession signals for a field of 80 G at room temperature and at 10K after zero-field cooling (ZFC). The enhanced relaxation rate at 10K is obvious. The solid lines are the results of fits made to a Gaussian relaxation function, $G_{xx}(t) = \exp - (\Delta t)^2$, which corresponds to a Gaussian distribution of internal fields.⁽⁷⁾ The low field in these spectra is convenient for illustrative purposes, but for measurements of λ , we used an external field $H_{ext} = 4\text{kG}$, which is well above H_{c1} ($\approx 150\text{G}$ at 10K, from other measurements^(3,4) in addition to our data described below) and well below H_{c2} for $T < 35\text{K}$.⁽⁴⁾ Fig. 2 displays the muon depolarization rate Λ as a function of increasing temperature after cooling in an external field of 4 kG. Above $T_c = 37\text{K}$, the fitted Λ , which is due to static nuclear dipole relaxation, is small ($0.102(2) \times 10^6 \text{ s}^{-1}$); below T_c , Λ increases by an order of magnitude, indicating that the internal field becomes more inhomogeneous as the superconducting state is entered. NMR⁽⁹⁾ and μ SR⁽¹⁰⁾ experiments on other type II superconductors have revealed the same effect, due to the vortex lattices formed when the external field penetrates the materials. The mean square inhomogeneity in the field sampled by the muons in μ SR or nuclear spins in NMR is⁽⁹⁾

$$\langle |\Delta H|^2 \rangle = \frac{H_{ext}^2}{4\pi} \left(\frac{d}{\lambda} \right)^2 \left[1 + \left(\frac{2\pi\lambda}{d} \right)^2 \right]^{-1} \quad (1)$$

where λ is the London penetration depth and d is the spacing between vortices. For the two-dimensional vortex array assumed in the derivation of eq. (1), $d^2 = \phi/H_{ext}$ where ϕ is the magnetic flux quantum, $2.068 \times 10^{-7} \text{ G-cm}^2$, so that

eq. (1) can be rewritten as

$$\langle |\Delta H|^2 \rangle = \frac{H_{\text{ext}} \phi}{4\pi\lambda^2} \left(1 + \frac{4\pi^2\lambda^2 H_{\text{ext}}}{\phi} \right)^{-1}. \quad (2)$$

Because $\Lambda\sqrt{2} = \gamma_{\mu} \langle |\Delta H|^2 \rangle^{1/2}$ ($\gamma_{\mu} = 2\pi \times 13.55 \text{ MHz/kG}$ is the gyromagnetic ratio of the muon), eq. (2) implies that λ can be extracted from μSR data. In particular, for high fields, $d \ll \lambda$ and eq. (2) becomes $\Lambda [\mu\text{s}^{-1}] \approx (2364/\lambda [\text{\AA}])^2$. For $\text{La}_{1.85}\text{Sr}_{0.15}\text{CuO}_4$, the corresponding value for λ at 6K is 2500 \AA , which is comparable to those of A15 compounds such as Nb_3Sn and V_3Si . It is also not far using what may be obtained using estimated values⁽¹¹⁾ of $K (= \lambda/\xi_0 \approx 100)$ and $\xi_0 (\approx 30\text{\AA})$, where ξ_0 is the coherence length. In type II superconductors, the London formula gives an approximate value for λ ,

$$\lambda = \left[\frac{m^*}{4\pi n_s e^2 c^2} \right]^{1/2} = \left[\frac{m^*/m_e}{4\pi n_s r_e} \right]^{1/2}, \quad (3)$$

where $r_e = e^2/me^2 = 2.82 \times 10^{-5} \text{ \AA}$ is the classical radius of the electron, m^* is the effective carrier mass, and n_s is the superfluid density, which, for ordinary superconductors at $T = 0$, is identical to the carrier density (n) for $T > T_c$.

The Sommerfeld constant can also be expressed in terms of m^* and n ,

$$\gamma = k_B^2 [\pi/3]^{2/3} m^* n^{1/3} / \hbar^2. \quad (4)$$

Simultaneous solution of eqs. (3) and (4), using the measured values of λ and $\gamma (\approx 6 \text{ mJ/mole-K}^2$ from ref. [4]) yields a small n , 0.3×10^{22} carriers/cm³, (≈ 0.3 carriers/formula unit), and a sizeable m^*/m_e , 7. For the band structure

of Matheiss,⁽¹²⁾ n ($\approx 10^{22}$ carriers/cm³) is larger and m^*/m_e (~ 3.5) somewhat smaller. Comparison of our result for m^*/m_e and that of Matheiss indicates that the electron-phonon coupling strength λ_{e-ph} in $\text{La}_{1.85}\text{Sr}_{0.15}\text{CuO}_4$ is not unusually large; indeed, λ_{e-ph} is of order unity, in agreement with a recent calculation.⁽¹³⁾ We emphasize that our values for n and m^*/m_e are merely estimates based on eqs. (3) and (4); it remains to be seen whether the uncorrected London formula is valid for samples such as ours.

Fig. 2(b) shows the temperature dependence of λ computed from Λ and eq. (2). Attempts to fit the present data to the form,

$$\lambda(T) = \lambda(0) (1 - (T/T_c)^4)^{1/2}, \quad (5)$$

which generally describes the behavior of ordinary superconductors, failed. The failure can be due to inhomogeneities, which lead to a distribution of T_c 's, or to the pressed powder's granularity, which causes percolation, finite size, and weak link effects.^(1,4) We note also that when the electronic mean free path ℓ becomes comparable to ξ_0 , which might well be the case for $\text{La}_{1.85}\text{Sr}_{0.15}\text{CuO}_4$,⁽¹⁴⁾ the standard expressions, eqs. (3) and (5), for $\lambda(0)$ and $\lambda(T)$ become invalid.⁽⁵⁾

Fig. 3 displays the field dependence of Λ for several temperatures and sample histories. Upon decreasing H_{ext} at $T=10\text{K}$, Λ is essentially field-independent until $H_{ext} \approx H_{c1} = 150$ Gauss, as it should be according to eq. (2). Subsequent reductions in H_{ext} lead to a monotonic decrease in Λ . Due to flux pinning and finite size effects, some flux still penetrates for $H_{ext} < H_{c1}$. The hysteresis in Λ (see fig. 3) is clear evidence for flux pinning at 10K. The near reversibility of

the 30K results indicates that there is considerably less flux pinning at higher T.

The zero field (ZF) and longitudinal field (LF) μ SR techniques measure $G_{zz}(t)$, the relaxation of the muon polarizations component parallel to the initial muon spin direction (\hat{z}); muons are depolarized only by fields with components perpendicular to \hat{z} . After cooling the sample to 10K in zero field (ZFC), we observe a slowly decaying ZF relaxation function indistinguishable from that found at 60K and well-described by a Gaussian Kubo-Toyabe form.⁽¹⁵⁾ Quite different behavior obtains after cooling the sample to 10K (from 50K) in a field of 4 kG applied along \hat{z} and subsequently removing the field (FC). Here, the zero-field relaxation is rapid and $G_{zz}(t)$ resembles a Lorentzian Kubo-Toyabe function.⁽¹⁵⁾ We conclude that the ZF relaxation after ZFC is due to static nuclear dipole moments, while the ZF relaxation after FC is derived from trapped flux lines with components perpendicular to \hat{z} . The LF measurements also demonstrate the existence of H_{ext} -induced internal fields transverse to \hat{z} . To understand such results, it is important to recall that a vortex lattice in which the flux lines are parallel to H_{ext} cannot enhance the LF relaxation. Indeed, we expect that in the normal vortex core regions, H_{ext} will serve to quench any such relaxation. This familiar decoupling effect, where $\lim_{t \rightarrow \infty} G_{zz}(t)$ increases rapidly with H_{ext} because H_{ext} serves to maintain the initial muon polarization, was described by Kubo and Toyabe and has been observed in many LF- μ SR experiments on non-superconducting materials.^(15,16) Comparison of the ZF and LF relaxation functions at 10K shows that the expected decoupling also occurs for superconducting $La_{1.85}Sr_{0.15}CuO_4$. However, as

shown in Fig. 4 the initial Gaussian relaxation rate increases monotonically with H_{ext} until $H \approx H_{c1} = 150$, beyond which it appears to be field-independent. The latter result is anticipated for the vortex state, while the original increase is probably due to flux lines forced to bend around small superconducting grains, thus generating transverse local fields with amplitudes roughly proportional to H_{ext} .

In summary, we have measured the magnetic penetration depth in the high T_c superconductor, $\text{La}_{1.85}\text{Sr}_{0.15}\text{CuO}_4$. The result at 8K, $\lambda = 2500\text{\AA}$, taken together with earlier thermodynamic measurements⁽⁴⁾, indicates a low density of carriers in this oxide. The temperature dependence of λ is inconsistent with the standard form for ordinary superconductors, a result which is hardly surprising when the morphology and chemical nature of the sample are considered. Our LF- μ SR measurements demonstrate the existence of random internal fields, induced by $H_{\text{ext}} < H_{c1}$ but with components perpendicular to H_{ext} . Thus, μ SR is a useful probe not only of λ for $H \gg H_{c1}$, but also of internal field distributions for $H < H_{c1}$ in inhomogeneous samples such as our sintered powder specimen.

Acknowledgements

We thank B. Batlogg, D. Harshman, and W. Weber for helpful discussions. Research at TRIUMF is supported by the Natural Sciences and Engineering Research Council of Canada and, through TRIUMF, by the Canadian National Research Council. One of the authors (GA) is very grateful to TRIUMF for its

kind hospitality when this experiment was performed.

References

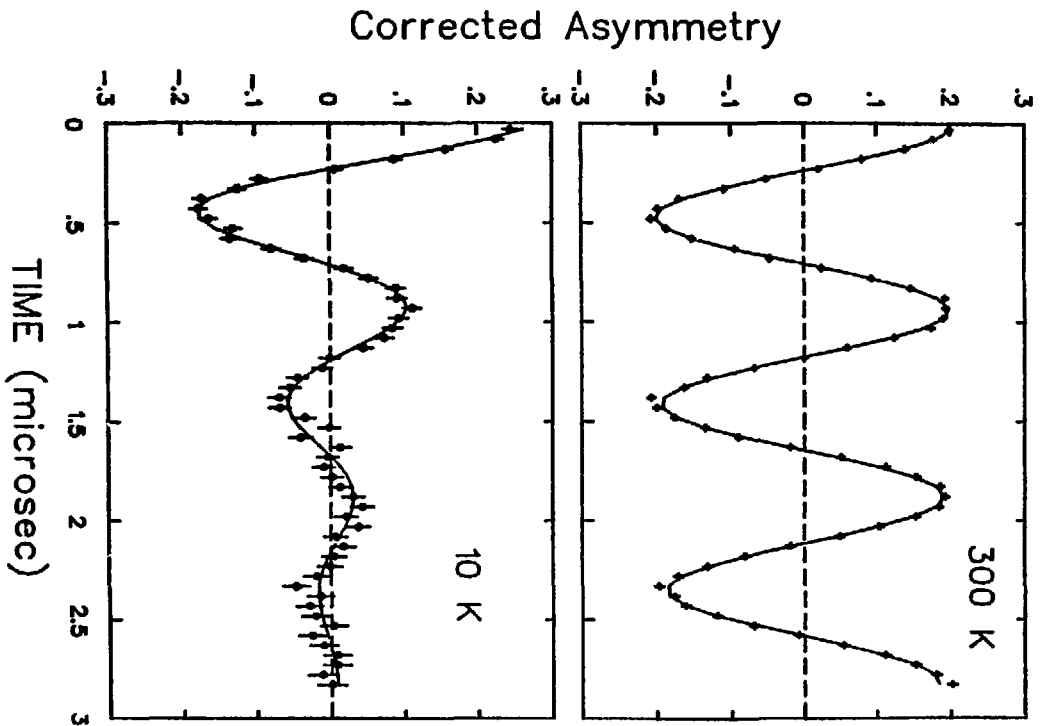
1. J. G. Bednorz and K. A. Müller, *Z. Phys. B* **64**, 189 (1986).
2. K. Kishio, K. Kitazawa, S. Kanbe, I. Yasuda, N. Sugii, H. Takagi, S. Ichida, K. Fueki, and S. Tanaka, *Chem. Lett.* submitted (1986).
3. R. J. Cava, R. B. van Dover, B. Batlogg, and E. A. Rietman, *Phys. Rev. Lett.* **58**, 408 (1987).
4. B. Batlogg, A. P. Ramirez, R. J. Cava, R. B. van Dover, and E. A. Rietman, preprint (1987).
5. M. K. Wu, J. R. Ashburn, C. J. Torng, P. H. Hor, R. L. Meng, L. Gao, Z. J. Huang, Y. Q. Wang, and C. W. Chu, *Phys. Rev. Lett.* **58**, 908 (1987).
6. For a review of early work on London penetration depths, see B. S. Chandrasekhar (p. 1) and R. Meservey and B. B. Schwarz (p. 117) in *Superconductivity I*, ed. R. Parks (Marcel Dekker, NY; 1969).
7. A. Shenck, *Muon Spin Rotation Spectroscopy: Principles and Applications in Solid State Physics* (Adam Hilger Ltd., Bristol and Boston; 1985).
8. J. H. Brewer, S. R. Kreitzman, D. R. Noakes, E. J. Ansaldo, D. R. Harshman, and R. Keitel, *Phys. Rev.* **B33**, 7813 (1986).
9. P. Pincus, A. C. Gossard, V. Jaccarino, and J. Wernick, *Phys. Lett.* **13**, 21 (1964).
10. A. T. Flory, D. E. Murnick, M. Leventhal, and W. J. Kossler, *Phys. Rev. Lett.* **33**, 969 (1974); Y. J. Uemura, W. J. Kossler, B. Hitti, J. R.

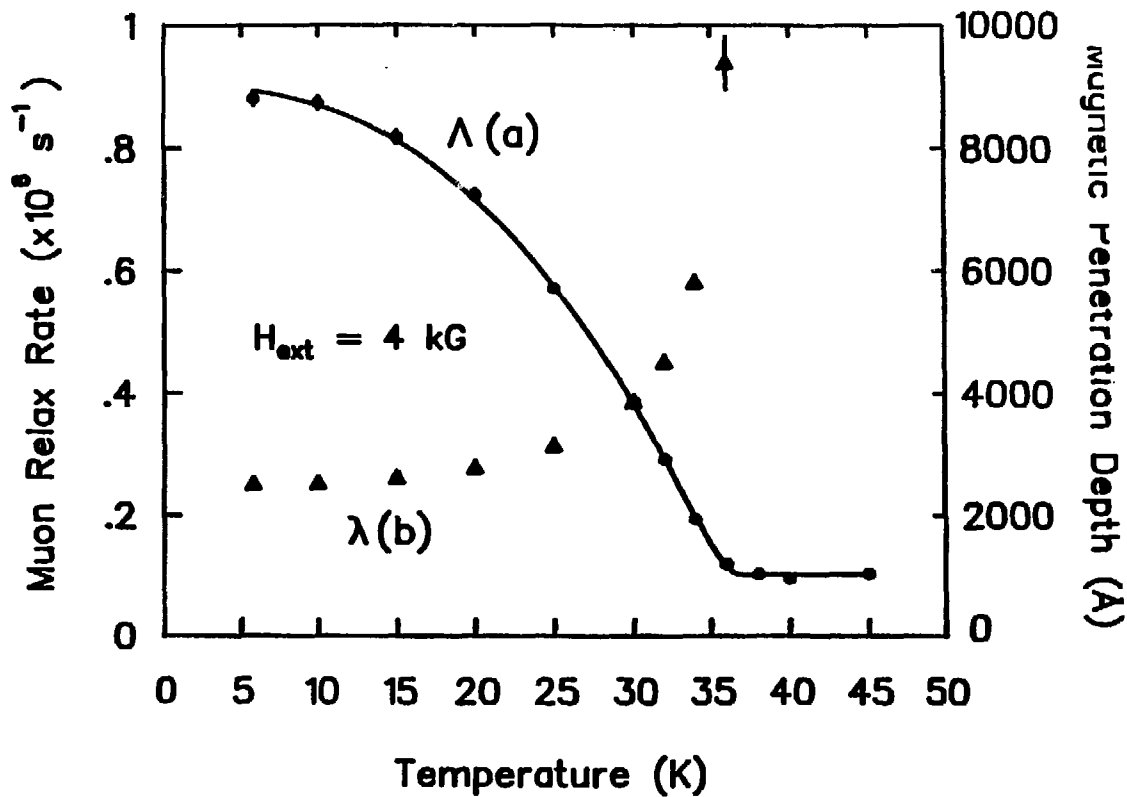
Figure Captions

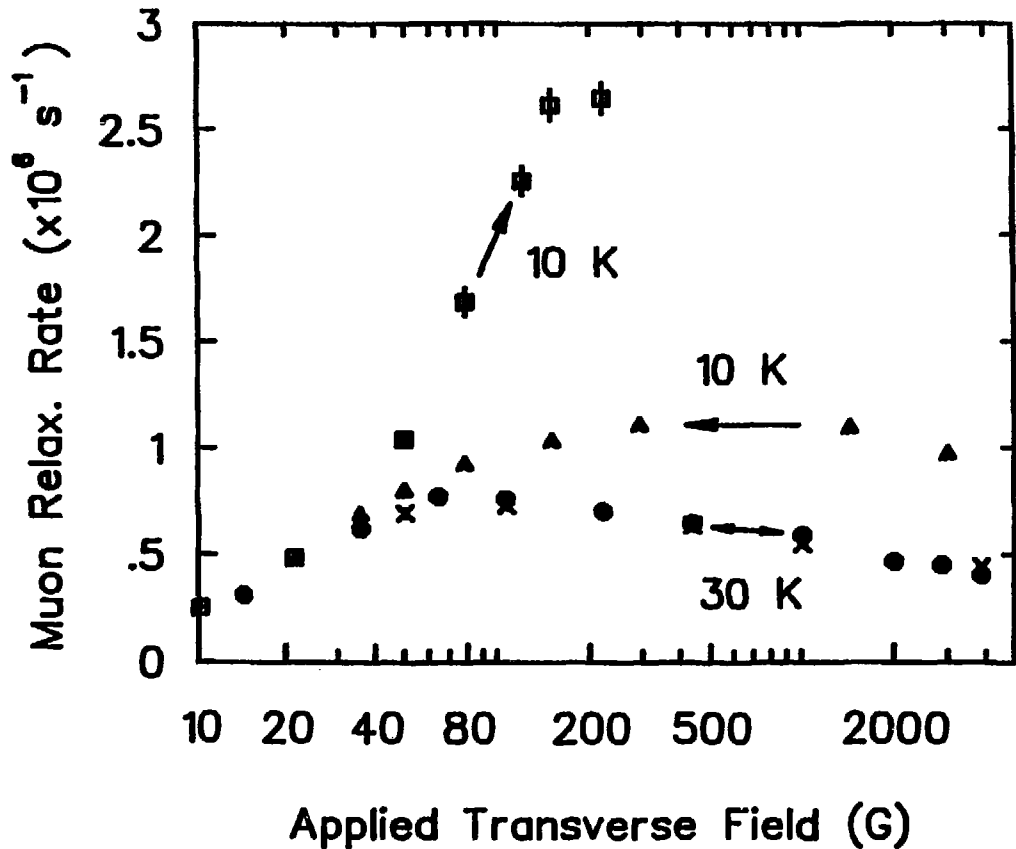
- Fig. 1. Muon spin relaxation signal in a transverse field of 80 G for T above and below $T_c = 37$ K. The 10K data were obtained after cooling in a 4kG field.
- Fig. 2. Temperature dependence of (a) [circles] the gaussian relaxation rate Λ obtained for a transverse $H_{ext} = 4$ kG after cooling in zero applied field; and (b) [triangles] the magnetic penetration depth λ inferred from Λ using Eq. (2) after correcting for a fixed nuclear dipolar relations rate $\Lambda_0 = 0.102(2) \times 10^6 \text{ s}^{-1}$, assumed to add in quadrature with the depolarization rate due to the vortex lattice. The solid curve is a guide to the eye.
- Fig. 3. Dependence of muon spin depolarization rate on transverse field strength for various temperatures and sample histories.
- Fig. 4. Dependence of the fitted value of the Gaussian relaxation rate (a measure of the mean squared internal field transverse to the applied field) found upon increasing the external field after zero-field cooling to $T = 10$ K.

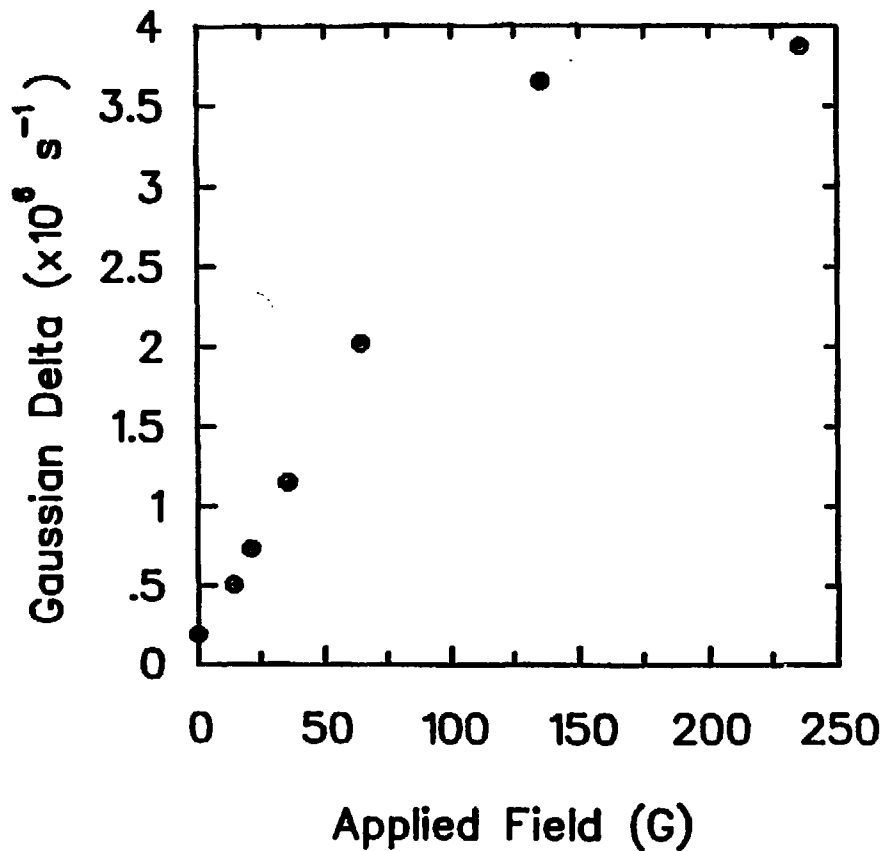
- Kempton, H. E. Schone, X. H. Yu, C. E. Stronach, W. F. Lankford, D. R. Noakes, R. Keitel, M. Senba, J. Bresler, E. J. Ansaldo, Y. Oonuki, T. Komatsubara, G. Aeppli, and E. Bucher, *Hyperfine Interactions* **31** 413 (1986).
11. B. Batlogg, private communication.
 12. L. F. Matheiss, preprint (1987).
 13. W. Weber, preprint (1987).
 14. W. W. Kwok, G. W. Crabtree, D. G. Hinks, D. W. Capone, J. D. Jorgenson, and K. Zhang, preprint (1987).
 15. R. Kubo and T. Toyabe (p. 810) in *Magnetic Resonance and Relaxation*, ed. R. Blinc (North-Holland, Amsterdam, 1967);
 16. R. S. Hayano, Y. J. Uemura, J. Imazato, N. Nishida, T. Yamazaki, and R. Kubo, *Phys. Rev. B* **20** 856 (1979).
 17. J. H. Brewer, S. R. Kreitzman, K. M. Crowe, C. W. Clawson and C. Y. Huang, *Phys. Lett. A*, in press (1987).

TF = 80 G









RCDC Bibliographic Database

The Radiation Chemistry Data Center maintains a database covering the literature on processes initiated by radiation or light. The database emphasizes kinetic and spectroscopic properties of radicals and other transient chemical species. The *Biweekly List of Papers on Radiation Chemistry and Photochemistry* is a current-awareness service derived from the RCDC Bibliographic Database. Studies involving muonium are of interest for inclusion in the database; for that purpose it would be appreciated if authors would forward reprints of their papers to the Center. For information on subscriptions to the Biweekly List or other services and activities of the Center write to:

Dr. Alberta B. Ross
Radiation Chemistry Data Center
Radiation Laboratory
University of Notre Dame
Notre Dame, IN 46556, USA